Bull Volcanol (2007) 69:741–756
DOI 10.1007/s00445-006-0103-4

RESEARCH ARTICLE

Pits, rifts and slumps: the summit structure of Piton de la Fournaise

Adam Carter · Benjamin van Wyk de Vries · Karim Kelfoun · Patrick Bachèlery · Pierre Briole

Received: 27 June 2005 / Accepted: 20 July 2006 / Published online: 22 November 2006

Abstract A clear model of structures and associated stress fields of a volcano can provide a framework in which to study and monitor activity. We propose a volcano-tectonic model for the dynamics of the summit of Piton de la Fournaise (La Reunion Island, Indian Ocean). The summit contains two main pit crater structures (Dolomieu and Bory), two active rift zones, and a slumping eastern sector, all of which contribute to the actual fracture system. Dolomieu has developed over 100 years by sudden large collapse events and subsequent smaller drops that include terrace formation. Small intra-pit collapse scars and eruptive fissures are located along the southern floor of Dolomieu. The western pit wall of Dolomieu has a superficial inward dipping normal fault boundary connected to a deeper ring fault system. Outside Dolomieu, an oval extension zone containing sub-parallel pit-related fractures extends to a maximum distance of 225 m from the pit. At the summit the main trend for eruptive fissures is N80°, normal to the north–south rift zone. The terraced structure of Dolomieu has been reproduced by analogue models with a roof to width ratio of approximately 1, suggesting an original magma chamber depth of about 1 km. Such a chamber may continue to act as a storage location today. The east flank has a convex–concave profile and is bounded by strike-slip fractures that define a gravity slump. This zone is bound to the north by strike-slip fractures that may delineate a shear zone. The southern reciprocal shear zone is probably marked by an alignment of large scoria cones and is hidden by recent aa lavas. The slump head intersects Dolomieu pit and may slide on a hydrothermally altered layer known to be located at a depth of around 300 m. Our model has the summit activity controlled by the pit crater collapse structure, not the rifts. The rifts become important on the mid-flanks of the cone, away from pit-related fractures. On the east flank the superficial structures are controlled by the slump. We suggest that during pit subsidence intra-pit eruptions may occur. During tumescence, however, the pit system may become blocked and a flank eruption is more likely. Intrusions along the rift may cause deformation that subsequently increases the slump's potential to deform. Conversely, slumping may influence the east flank stress distribution and locally control intrusion direction. These predictions can be tested with monitoring data to validate the model and, eventually, improve monitoring.

Keywords Fracture · Pit crater · Rifting · Slumping · Shield volcano · Piton de la Fournaise · Digital elevation model

Editorial resposibility: A Harris

A. Carter (✉)
Department of Geology and Planetary Science,
University of Pittsburgh,
200 SRCC Building, 4107 O'Hara Street,
Pittsburgh, PA 15260-3332, USA
e-mail: ajc44@pitt.edu

A. Carter · B. van Wyk de Vries · K. Kelfoun
LMV, OPGC, Université Blaise Pascal,
5 Rue Kessler,
63000 Clermont-Ferrand, France

P. Bachèlery
LSTUR,
15 Avenue René Cassin, BP 7151,
97715 Saint Denis Cedex 9, Réunion, France

P. Briole
CNRS, IPGP,
4 Place Jussieu,
75005 Paris, France

Introduction

The origin of pit craters and volcanic subsidence mechanisms has been discussed previously for Hawaii (Okubo and Martel 1998) and Masaya, Nicaragua (Rymer et al. 1998). Roche et al. (2001) took such studies further by applying analogue model results to summit pit crater structure and dynamics at such volcanoes as Kilimanjaro (Tanzania), Telica and San Cristobal (Nicaragua), and Ubinas (Peru). Bachèlery (1981) made a comprehensive analysis of the summit fracture system of Piton de la Fournaise (La Reunion Island, Indian Ocean) and suggested a strong linkage between the crater structure and the rift zones. Small-scale pit collapse events share many similarities with larger caldera collapses, as seen in scaled analogue models (Walker 1988; Roche et al. 2001; Walter and Troll 2001). We take a similar approach to Roche et al. (2001) and build on the work by Bachèlery (1981) to study the summit structure of Piton de la Fournaise, but integrate new structural data from zones outside the pits. This includes field data for features such as fractures, eruptive fissures, and flank morphology. We use these data in comparison with analogue experiments to explore the links between summit pit craters, rift zones, and possible gravity- or dyke-driven slumping on the eastern flank. We use this improved structural knowledge to provide a model for the eruptive system mechanics.

Piton de la Fournaise

Piton de la Fournaise is a highly active oceanic shield volcano located on the southeast of La Reunion Island (21°S, 55.3°E), 750 km east of Madagascar (Fig. 1a and b). The oldest parts of the volcano are dated at about 0.53 Ma (Gillot et al. 1990). The current average repose time is approximately 10 months, with around 125 eruptions recorded in the last century. Around the centre of the volcano the Enclos Fouqué cliff surrounds the summit and continues down to the coast to make a horseshoe shape (Fig. 1c). The 400 m high summit cone (altitude 2,631 m) is approximately 3 km in basal diameter and is thought to be around 3,000 years old (Bachèlery 1981). At the summit there are two pit craters: Bory (ca. 250 m north–south by 175 m east–west) and Dolomieu (ca. 725 m north–south by 1,125 m east–west, Fig. 1d). The east section of Bory has been partly destroyed by collapse and opens into the larger Dolomieu pit to the east. Dolomieu has a flat interior and cliff walls 50–160 m high in the east and west, respectively.

Flank eruptions are concentrated along a diffuse arcuate rift zone (N10 and N170°), with 97% of eruptions occurring within the Enclos Fouqué caldera. Historical eruptions were also concentrated along a N120° rift

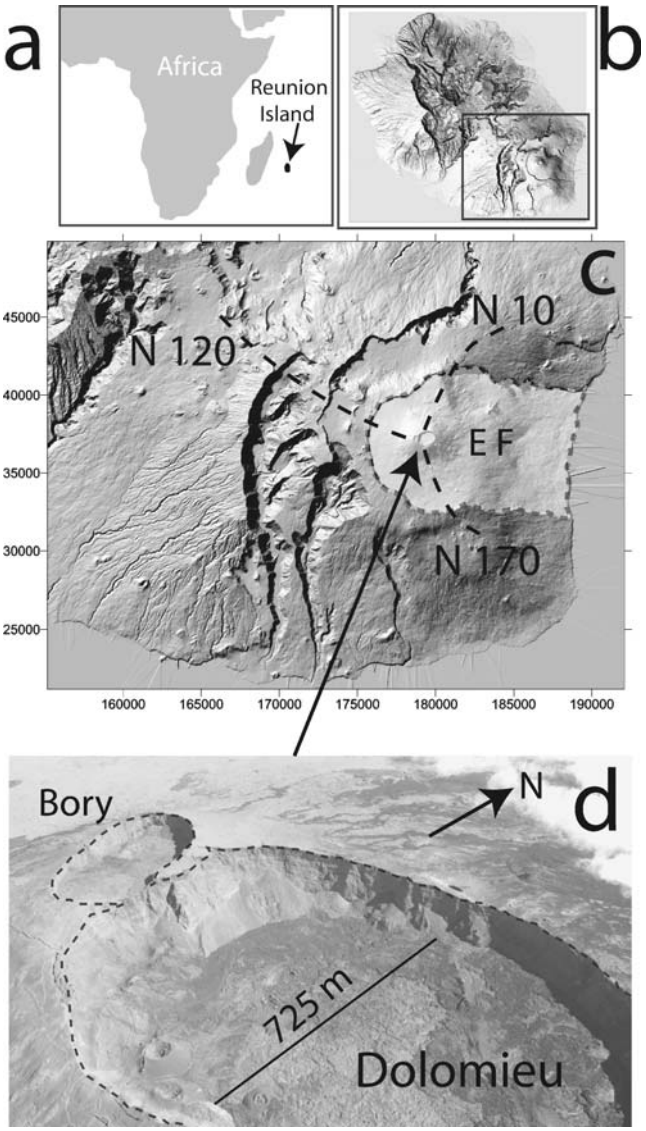

Fig. 1 **a** Geographic setting of La Reunion Island, in the Indian Ocean. **b** La Reunion Island, *box* covers the area of Piton de la Fournaise for Fig. 1c. **c** Shaded relief map showing the principal rift zones (N10, N120, N170°). The summit cone (marked with an *arrow*) is within the Enclos Fouqué caldera (EF, delineated by *small dashed lines*), which opens out to the east. Gauss–Laborde projection in metres. **d** Aerial photograph looking northwest of the smaller Bory pit crater and Dolomieu (*foreground*) taken in April 2002

(Bachèlery 1981). The summit region is entirely covered by volcanic products, with vegetation only growing at lower altitudes. The composition of all products is basaltic (Gillot et al. 1990). There are both aa and pahoehoe lavas on the summit cone as well as blocks that were emplaced near to the summit pits during phreatic and phreatomagmatic events. Frequent eruptions rapidly resurface older structures; however, flows from the eighteenth century are still visible on the northwest flank (Lénat et al. 2001).

Historical accounts

Historical records of summit events are rare; however, Bory de St. Vincent (1804) provided several sketches and descriptions of volcanism at the time. His descriptions included one volcanic centre at the summit with an east flank eruption in 1760, followed by an elongation of the summit cone by a new eruptive centre to the east in 1775. The summit centre was inactive at the time of a sketch made in 1775. In 1789, both the 1760 eruptive centre and the western centre (Bory) were synchronously eruptive, but by 1791 only the easterly centre was active, with activity located at a vent lower down on the east flank. A phreatomagmatic eruption in 1791 accompanied the formation of a collapse structure that was 200 m in diameter and 40 m in depth. This has been interpreted as the beginning of the formation of the pre-Dolomieu pit complex (Bachèlery 1981).

In 1801, eruptions were concentrated on the east part of the summit cone, with a minor vent constructed between the eruptive area and the then non-eruptive Bory crater. This 50 m high vent was named "Mammelon Central" and existed until around 1820, at which point it collapsed to create a collapse structure within the western part of Dolomieu (Lacroix 1936; Lénat et al. 2001). Dolomieu pit has alternately grown deeper by collapse and more shallow by successive lava infilling, with complete filling of the pit observed in 1844, 1859, 1874, and most recently in 1911 (Bachèlery 1981). Bory de St. Vincent also observed lava lakes at the summit in 1801 and 1852. The eighteenth century cone began to enlarge eastwards around 1760–1801 and probably developed a new shallow intrusive system. This began to form the intrusion which triggered the Dolomieu pit structure. This, in turn, was fully developed by 1936 and is still actively changing.

Each larger pit crater collapse was often associated with a significant fissure eruption, followed by phreatic and phreatomagmatic explosions. These explosions have been recorded in 1760, 1766, 1791, 1802, 1812, and 1860 (Kornprobst et al. 1984; Delorme et al. 1989). Angular blocks can be found up to 200 m from the pit craters and are generally light in colour due to hydrothermal alteration.

1911–present day

Accounts from 1911 onwards are more complete and the subsequent major events have been well documented (Fig. 2a, adapted after Bachèlery 1981). In 1911, Bory was the only pit at the summit. To the east there was a plateau, probably a result of infilling of pre-Dolomieu pits. In 1927, a small collapse about 100 m in diameter and several metres deep began on the east part of the plateau and propagated to the west, increasing in depth to 150 m in the early 1930**s**. Rapid subsidence of about 25 m/year was estimated between 1927 and 1936, probably linked to the estimated 130×10^6 m^3 of lava, which erupted in 1931 and significantly reduced the magma reservoir volume (Bachèlery 1981). This continued until 1933 when the Enclos Velain, a crescent-shaped plateau, collapsed vertically by 50 m into the west side of Dolomieu (Fig. 2b). A photo taken on the north flank of Dolomieu in 1935 (Lacroix 1936) shows the location of the intersection between the deepened eastern part of Dolomieu (sometimes called 'Brulant' Crater) and the Enclos Velain plateau raised above it. Lavas erupted around the Enclos Velain plateau and flowed into the lower part of Dolomieu. This progressively in-filled the Dolomieu pit, with the December 1985—January 1986 eruptions removing all surface evidence of the scar between Dolomieu and Enclos Velain. This scar is now at a depth of a few metres below the current pit floor. Dolomieu and Bory became connected around 1953, when the eastern wall of Bory fell into Dolomieu. A small pit crater formed in 1986 in southeast Dolomieu but was fully refilled by June 1987. There are several pit crater structures concentrated around the southern wall of Dolomieu, the most recently formed structure being the 2002 pit crater (Fig. 2b). This crater began to form after the December 2002 eruption in southwest Dolomieu, in the southern part of the Enclos Velain terrace. Concentric fractures within a 50 m radius of the pit centre were apparent in Dolomieu cross-cutting the flanks of a scoria cone to the east. The pit crater became the centre of an eruption that began on 30 May 2003, producing a lava flow that moved north inside Dolomieu with a total length of around 400 m. Tiltmeters showed radial inflation of the summit cone in the preceding months (Staudacher, 2003, personal communication).

Fractures of Piton de la Fournaise

Although features are readily apparent across pahoehoe surfaces, the chaotic, blocky aa lava often hides smaller fractures. Our data and analyses are therefore principally based on fractures within the pahoehoe lavas, which constitute about 60% of the surface of the summit cone. There are many small fractures in the lava flows. Often large lobes and lava fields have steep edges and increased fracturing occurs at flow edges and just outside the flow fields. Such features are probably related to loading from lava, cooling-related contraction, or inflation of pahoehoe flows (Murray 1988; Froger et al. 2004). On Piton de la Fournaise, we distinguish two major groups of fractures:

1. *Concentric fractures:* Bory and Dolomieu are surrounded by near-vertical (90±5°) concentric fractures that are roughly parallel to the pit walls. Most of the

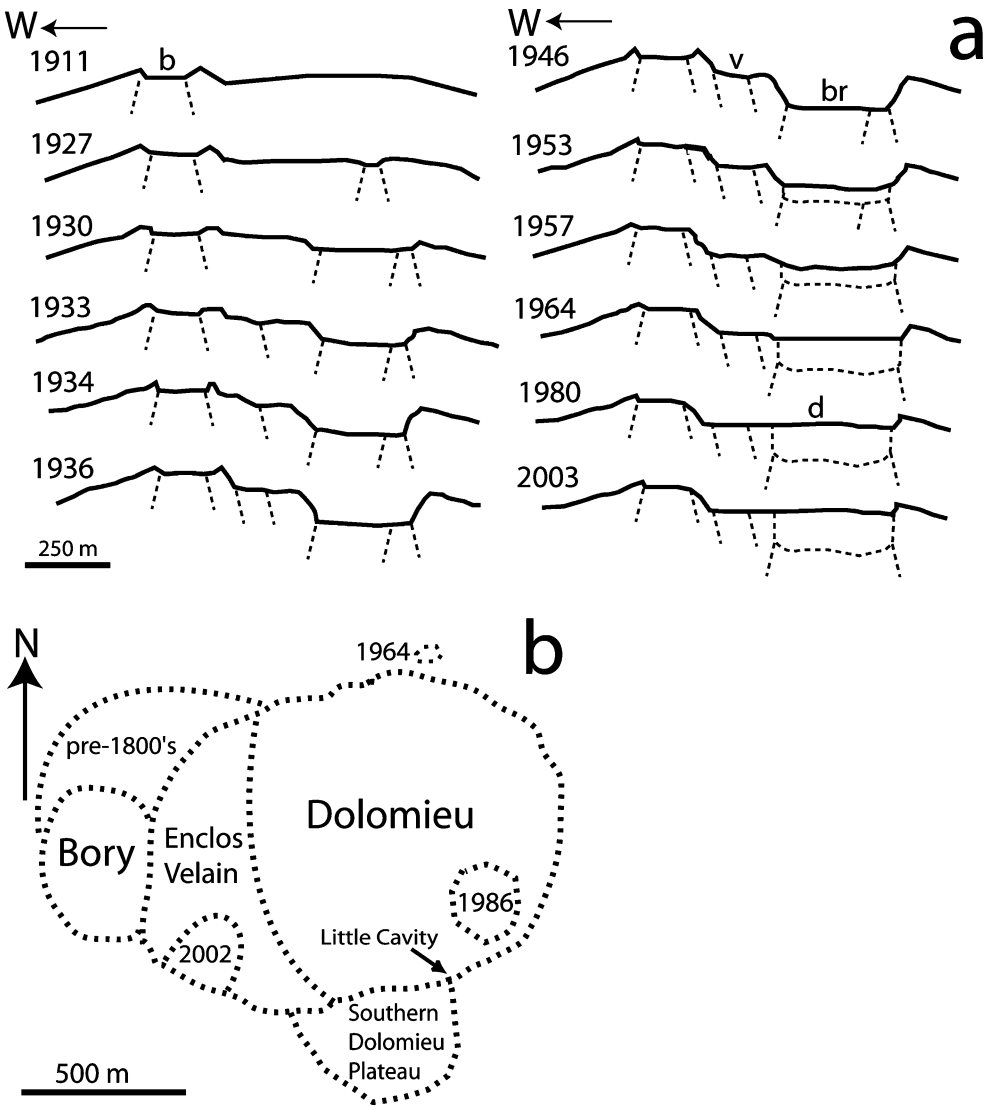

Fig. 2 **a** Summit evolution from 1911 to present. In 1911, Bory crater (*b*) was the only pit on the summit cone. In 1927, a small collapse began on the east part of the plateau and propagated west, increasing in depth to 150 m in the early 1930**s**. Enclos Velain (*v*) collapsed by 50 m to the west of Dolomieu (or Brulant (*br*) crater), forming between 1927 and 1936. Bory and Dolomieu became connected around 1953, followed by the progressive infilling of Dolomieu (*d*) to the present day. **b** Summit map showing all pit craters delineated by *dotted lines*. Bory and Dolomieu pit are separated by the Enclos Velain terrace, the eastern suture of which has been covered by more recent lavas. A break in slope on the northwest flank may be an older crater structure that was infilled by a large outpouring of lava during the eighteenth century. The Southern Dolomieu Plateau delineates a flat area originating from an infilled crater, with the Little Cavity exposed in the Dolomieu walls nearby. The 1964 La Soufriere pit crater lies to the north of Dolomieu and is a deep bottle-neck shaped cavity. The 1986 pit crater on Dolomieu floor has now been covered, whereas the 2002 pit is still prominent within the Enclos Velain terrace

fractures are 'dry' (i.e. non-eruptive), but a few have served as conduits for fissure eruptions. Bory pit is also cross-cut by large north–south trending fractures probably related to the Dolomieu collapse (Bachèlery et al. 1983). The fractures up to 10 m from the crater edge probably formed from inward collapse of the pit cliffs. The outer fractures are too far away to be controlled by cliff instability and must be solely related to pit boundary fault movement.

2. *Eruptive fissures:* These are often radial to the central area of Dolomieu and are the principal feeding systems for eruptions (Bachèlery 1981; Lénat and Bachèlery 1990). The fissures are normally a maximum of 1–2 m wide and each segment can be several tens of metres long. The down-slope sections of eruptive fissures are invariably covered by spatter and lava and are not visible at the surface. Up-slope of the fissures, fractures begin as small cracks with parallel openings that widen towards the eruption site. Several fractures have an en-echelon arrangement. The lava flows have numerous channels and levée structures, which may appear similar to eruptive fissures when viewed from aerial photographs. It is difficult to fix the fissure terminus and the dimensions of the subsequent lava flow, as the two may overlap. The eruptive fissures are not always radial from the centre of Dolomieu; for example, the fissures of the northwest and west flanks of the summit cone follow the cone contours in places and could be considered concentric to the pits.

Materials and methods

Morphological studies

Large-scale slope morphology studies have been completed on Piton de la Fournaise using aerial photographs (Bachèlery 1981) and radar interferometry (Rowland and Garbeil

2000). For our study, a summit slope survey was carried out using the IGN (Institute Geographique National, France) 25 m resolution Digital Elevation Model (DEM) of the island. The aim was to highlight the larger-scale topographic features of the summit area. The analysis shows five distinct morphological zones:

1. The floor slope varies from 0 to 10° inside Dolomieu and Bory and is produced by lava flow infill (Lénat et al. 2001).
2. Low slope angles characterize the edges of the pit craters, coinciding with zones of concentric fractures.
3. There is a flat circular structure south of Dolomieu that is interpreted as an old crater, possibly the 1801 lava lake crater. This is named "Southern Dolomieu Plateau" (Fig. 2b) and has undergone collapse and subsequent infilling (Bachèlery 1981).
4. Satellite cones normally lie within the N10 and N170° branches of the north–south rift zone and appear as areas of increased slope. Additional cones follow a general eastern strike around the summit and are also found around the base of the summit cone, outside of the proposed rift zone.
5. There is a steep area on the east flank of the summit cone that spatially coincides with the area of greatest deformation during recent dyke intrusion episodes (e.g. Froger et al. 2004), and may be steepened by dyke-induced deformation. This area is the most likely to suffer slope instability.

Digital cartography of the summit fractures

Using an ortho-image (spatial resolution 1 m) created from photos taken from a summit over-flight during 1981, the fracture network has been mapped and organised into a Geographical Information System (GIS) (Fig. 3) to improve upon existing maps (Bachèlery 1981; Stieltjes 1985). It highlights the major fracture trends and shows segmentation of eruptive fissures which are often characterized by an en-echelon alignment. This map now provides an accurate digital reference for all future research on the fracture network, such as integration of the current self-potential network on La Reunion Island.

The fractures mapped around the summit are mostly radial or concentric. The rift zones are seen as moderate fissure concentrations. Several concentrations are observed. There is a zone of increased fracturing on the northeast side of the summit cone. Some fractures in this orientation continue to the northwest side of Dolomieu, where they appear to join the wall faults. There is a corresponding but less well developed band of eruptive fractures on the southeast flank that follows the N120° rift zone of Bachèlery (1981). The east flank has an evident conjugate fracture system, whilst the south side of the summit cone contains a prominent set of fractures parallel with the elongated sides of Dolomieu.

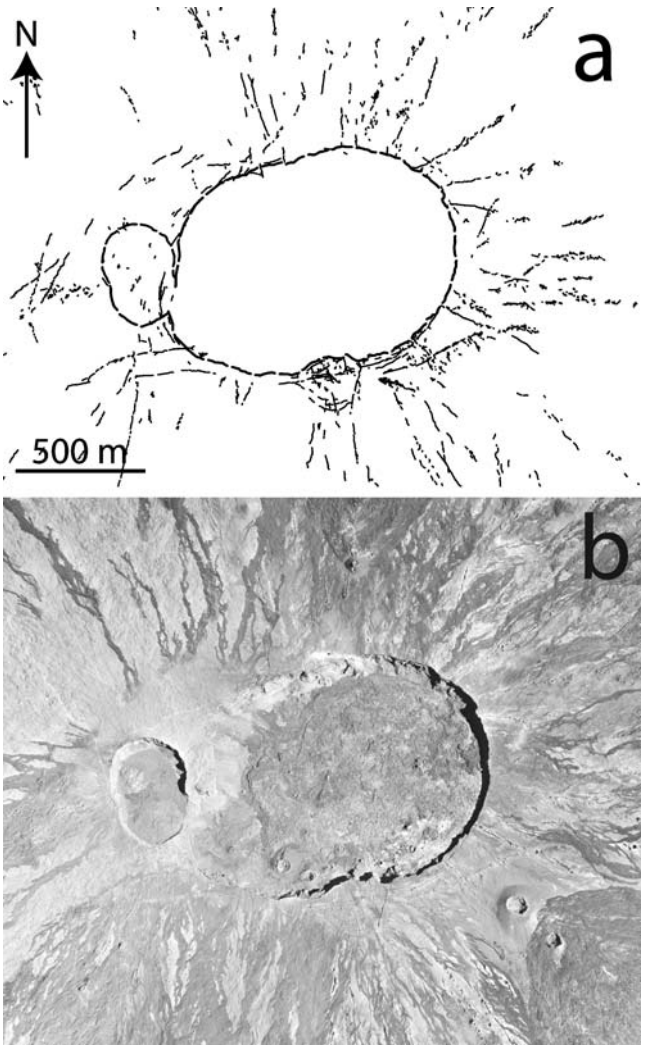

Fig. 3 **a** Digital map of traced fissure and fracture pattern from a 1981 ortho-image (courtesy of The Institute Physique du Globe, Paris). All fractures shown as *solid lines*, with pit boundaries as *dashed lines.* **b** 1981 over-flight ortho-image of the summit region

High-resolution DEM of the summit region

Using the oblique image stereo photogrammetry method of Kelfoun (1999), digital photograph pairs were used to produce several high-resolution DEMs for localized areas. The low-angle digital images were taken during an over-flight from a light aircraft in 2002. Images were located using an automatic calibration process based on known ground points and a bundle adjustment following Cecchi et al. (2003). All DEM data were then combined to produce a reconstruction of the summit topography at a 2 m horizontal resolution. A composite DEM (Fig. 4) with overlain ortho-images revealed surface features missing from the

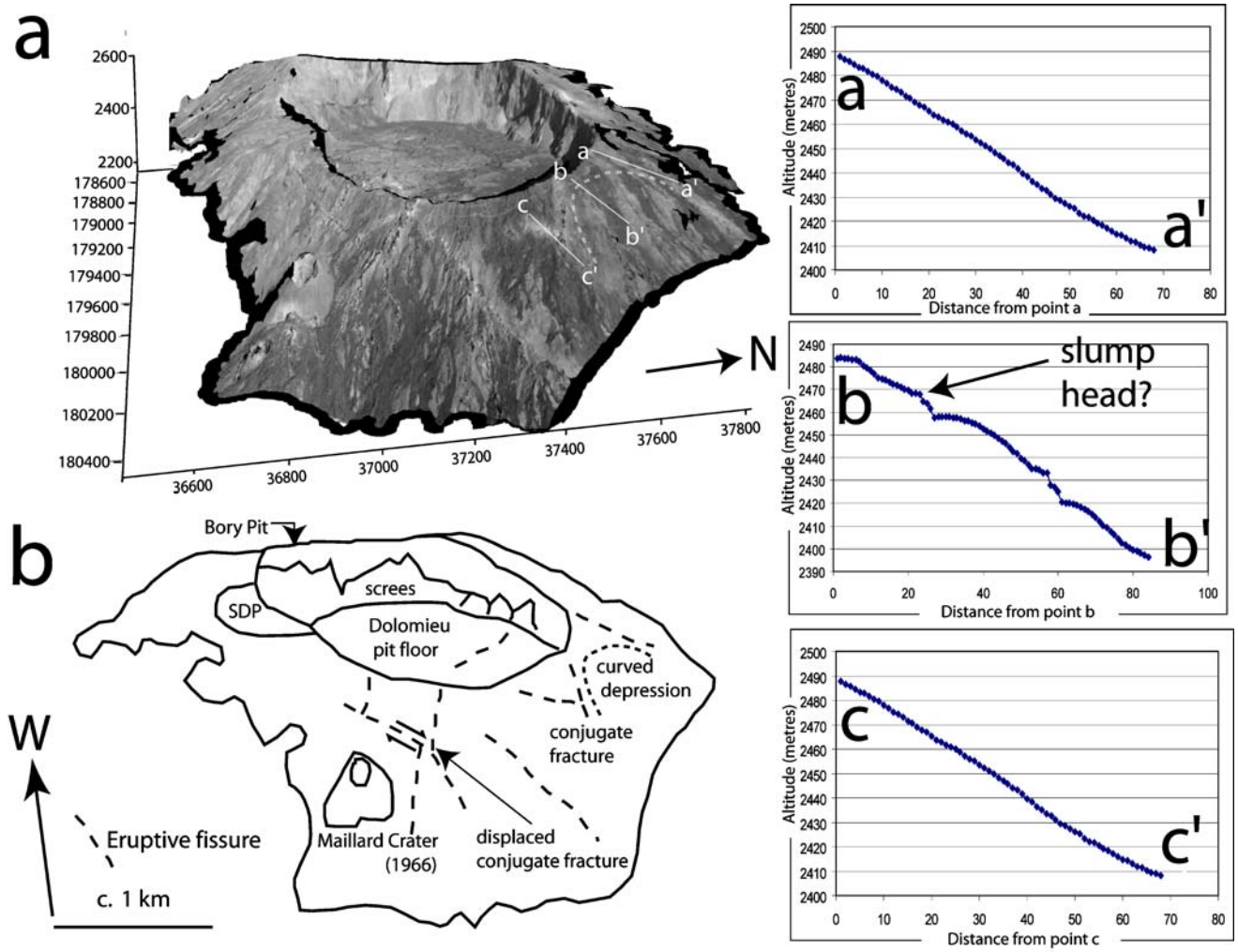

Fig. 4 **a** Ortho-image using 2002 photos overlain on a DEM of Dolomieu pit looking west (resolution 2 m). Gauss Laborde projection is in metres on the *x* and *y* axes. The altitude range is 2,200–2,600 m on the *z* axis. A previously unseen curved depression (*dashed line*) was found on the northeast flank on the DEM. Three 80 m long topographic profiles of this area (*a–a′*, *b–b′*, *c–c′*) show the probable position of the slump head in profile *b–b′*. **b** Synthesis of observations. *Low slope angles* can be found around the Southern Dolomieu Plateau (SDP) due to infilling of a crater. Conjugate fractures are apparent on the east flank, which have developed into eruptive fissures. One eruptive fissure shows right-lateral displacement after emplacement

lower resolution 25 m DEM. This included a curved depression on the eastern flank which may be the headwall of a small slump structure. This is also apparent in 80 m long topographic profiles across the feature (Fig. 4). This discovery highlighted the need for a ground-truth field study to map this area in more detail.

Field data

Following the initial remote sensing studies, field mapping was undertaken to inspect the structures and look at fractures beneath the resolution of the aerial photos. All of the non-eruptive fractures measured were within 225 m of the pit edges around Dolomieu and Bory or within the pits themselves. Dips of fractures were spread about 5° around vertical. However, they were rough-sided so that the measurement error on dip was quite high. Fracture data were compiled into a frequency distribution and rose diagrams (Fig. 5).

Non-eruptive fractures had preferential strike azimuths of N10, N50, N80, and N170° (Fig. 5b), with very few fractures at N110°. This shows that the non-eruptive fracture distribution is not entirely concentric around the pit crater systems. The eruptive fissures around the summit region show a preferential strike of N10, N50, N80, and N160° (Fig. 5c). The largest peak in strike frequency is around N80°, with two low concentrations on either side. The lowest fracture concentration lies on the axis N110°, which has no recorded eruptive fissures and very few non-eruptive fractures.

A close correlation exists in the preferred orientation of the eruptive and non-eruptive data sets, with frequency peaks in both fracture types that strike N10, N50, and N80°. The N10° group is aligned within the northeast branch of

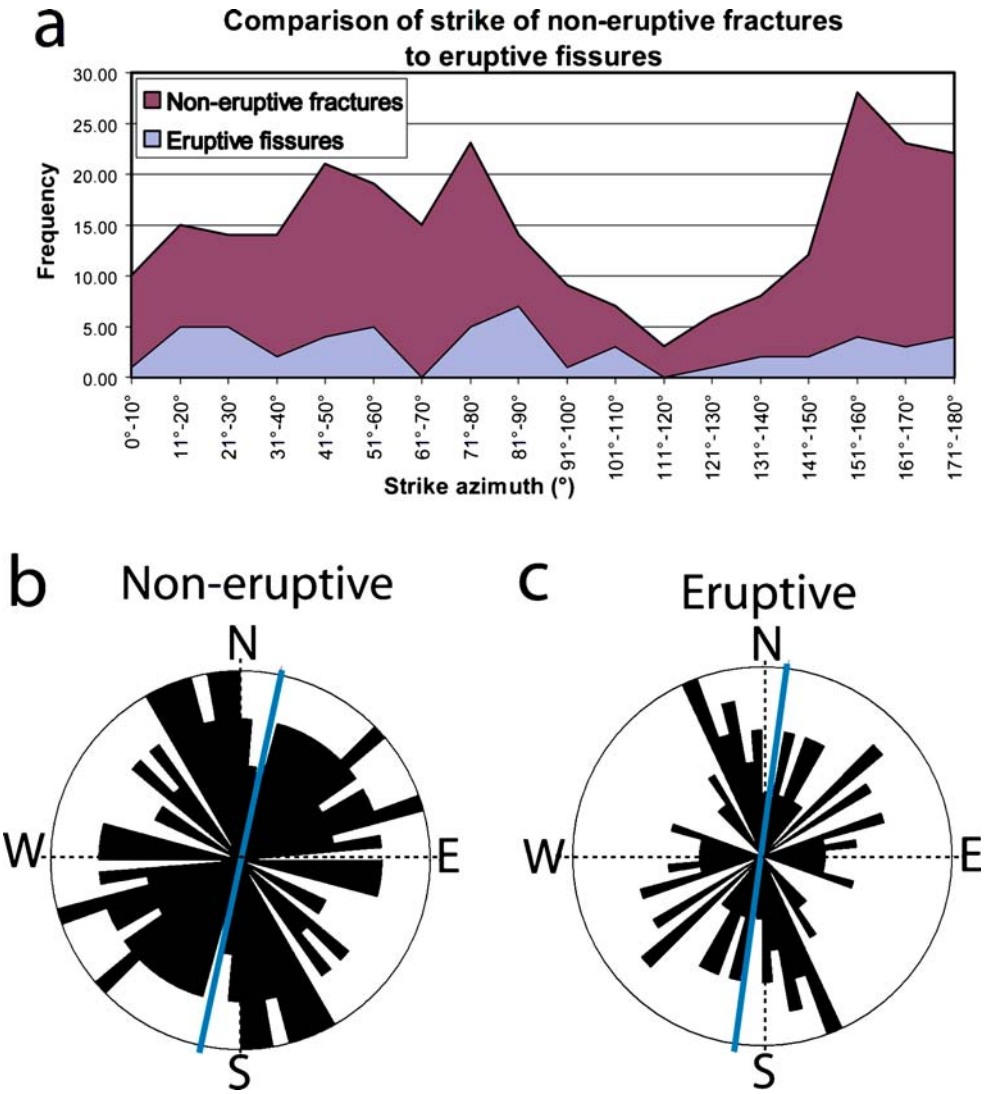

Fig. 5 **a** Frequency distribution of all fracture data for eruptive and non-eruptive fractures. **b** Rose diagrams of fracture azimuth distribution using a bi-directional (*mirrored*) presentation of non-eruptive fractures. Two hundred and thirty fracture measurements were taken and grouped into class sizes of five, giving a vector mean of 12.07 (*bold line*). Concentrations at N10, N50, N80 and N170° can be seen, and a minimum at N110°. **c** Eruptive fissures rose diagram. Fifty-four measurements were taken, grouped into class sizes of five, giving a vector mean of 7.77 (*bold line*). Concentration peaks are found at N10, N50, N80, and N170°, and a minimum at N110°. A distinct correlation in preferential azimuth distribution for the N10, N50, and N80° was observed, with a lack of data for both groups around N110°

the north–south rift zone and is probably linked with dykes rising along this zone. The N50° peak also may correspond to a preferential fracture orientation on the southwest flank, leading into Dolomieu pit and exiting with a strike azimuth of N80° (Bachèlery 1981). The N80° group is comprised of a set of long eruptive fissures that traversed the summit cone, with a concentration of fissures high on the south flank. Many of the concentric fractures are found predominantly at the north and south flanks around the oval Dolomieu pit to give a preferential concentration around N80°. Broad concentrations in strikes from N130 to N180° are roughly aligned with the southeast limb of the N170° rift zone. The rift zone and pit structures may account for most of the azimuth concentrations; however, the reason for the N110° gap in the data (Fig. 5a) remains unclear.

Detailed description of key areas

South Bory fracture zone This area includes the south part of the now buried Enclos Velain Terrace, which has been a structurally complex and active area over the last 100 years. It hosted several eruptions and is associated with smaller terraces tilting inwards toward Dolomieu pit, highlighting instability in this region (Fig. 6a). Elevated volcanic activity levels in this area continue to the present day. Several large fractures inside Bory continue onto the southwest flank of the summit cone. There is a concentration of fractures at the pit edge clearly associated with gravitational collapse of the walls. An area more than 10 m from the walls contains sub-parallel fractures that strike N340°. These vertical fractures may originate from the 1927 Dolomieu collapse and from the later Enclos Velain terrace collapse. Some fractures are down thrown to the east–northeast, with over 30 cm of total vertical displacement, leading towards Dolomieu (Fig. 6b). The fractures are tensional with an opening direction of approximately N75°. The configuration indicates a slight transtensional movement parallel to the long axis of Dolomieu pit crater. This type of fracturing suggests a network of fractures that propagates downwards into a fault with normal movement at depth. The easterly movement of

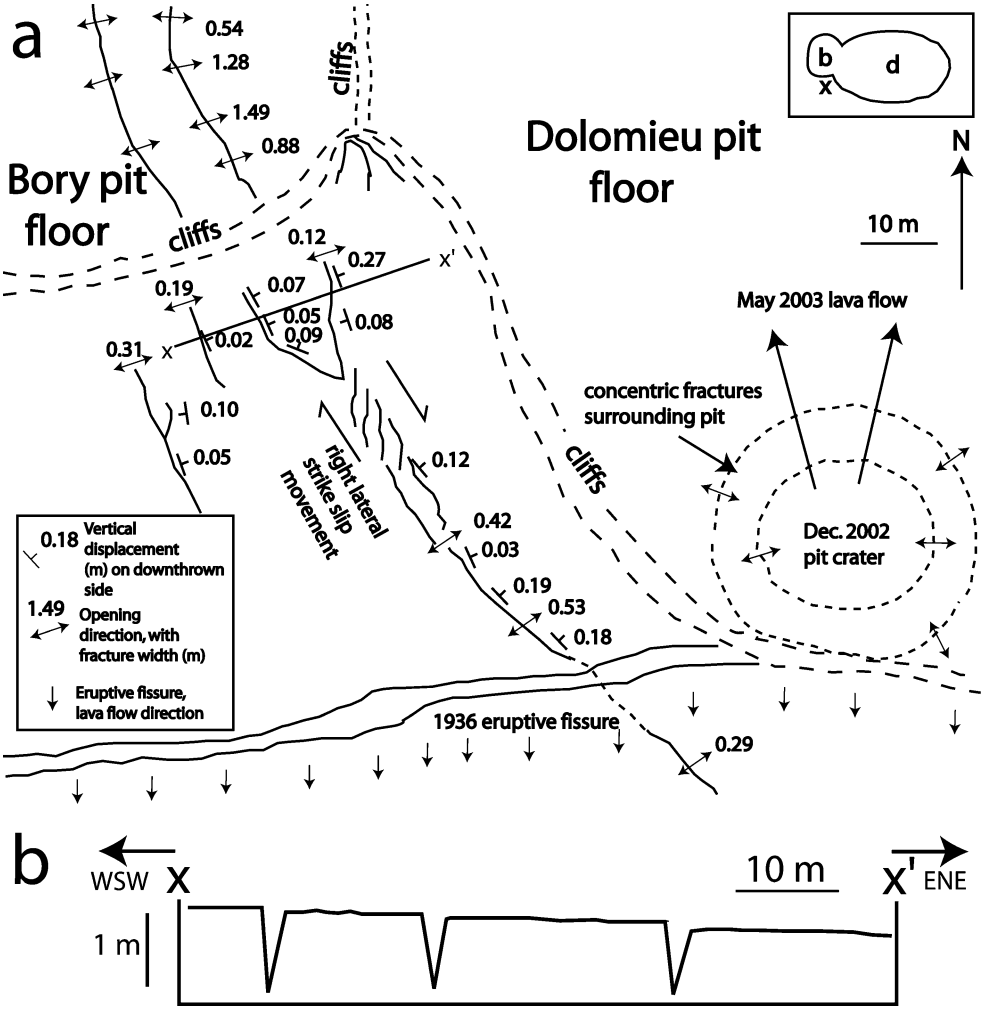

Fig. 6 **a** Southwest flank structural data map in plan view (see *top right corner* for location map relative to Bory and Dolomieu pits, marked with an *x*). Vertical displacements and fracture widths in metres, with fracture strike in degrees. Thirty-two fracture measurements were taken south of Bory and 36 measurements were taken within Bory itself. Dolomieu pit enlarged towards the west after 1927 and may have triggered the tearing of this area, creating mixed mode fractures south of Bory pit. Fractures were tensional and exhibited right-lateral strike-slip movement in en-echelon segments, showing slight down-faulting to the east. The 2002 pit crater is also located in this corner of Dolomieu, which became an eruptive vent in 2003. **b**. Sketch profile *x*–*x*′ shows a slight down-stepping of blocks by over 0.3 m towards the east–northeast

the terrace may have been transferred to strike-slip movements in the north and south Dolomieu areas. Bachèlery et al. (1983) suggested that the area north of Bory underwent left-lateral movement, opposite and complementary to the movement seen in the South Bory area. This suggested movement in the north Bory area was not observed during this field investigation, but some earlier fracturing may have been obscured by more recent lava flows.

The 'Little Cavity': evidence of stoping and pit crater formation The Southern Dolomieu Plateau intersects with the Dolomieu wall, leaving a section through the infilled pit crater exposed (located on Fig. 2b). Within this section there is a structure that we have called the Little Cavity (Fig. 7). This is a cylindrical depression with an arched roof. The inner walls of the cavity are brecciated in places, with loose blocks and scree lying on the Dolomieu pit floor. We interpret that this chaotic deposit was a product of stoping that formed before Dolomieu (thus before 1927), as this was that collapse event which exposed the Little Cavity in the pit walls. Such cavities were seen to form in the active pit at Masaya volcano (Rymer et al. 1998), and may have formed in the same way as the 1964 La Soufrère pit crater to the north of Dolomieu or the 2002 pit crater. They have also been observed at Telica, Nicaragua (Roche et al. 2001) and Hawaii (Walker 1988). The frequent formation of such small cavities and collapses suggests that they are typical features of pit crater evolution.

A highly fractured area on the northeast flank The northeast flank of Dolomieu has a zone of strong fracturing best developed in old pahoehoe surfaces, but also found within the recent aa lava flows (Fig. 8a). This zone extends as a broad band northeast from Dolomieu and is around 250 m wide. It was discovered following the creation of the GIS map of fractures (Fig. 3a). The fractures were parallel, with an average strike of N160°. The opening direction of N48° (northeast) was downslope. The fracture widths were below 0.5 m and lengths were several tens of metres. The opening vector, seen in offset pahoehoe lobes, is not perpendicular to the fracture strike and has a slight left-lateral component. Faint horizontal striae were observed on the fracture walls. These fractures had a rough direction when brushed with the hand and smooth in the opposite

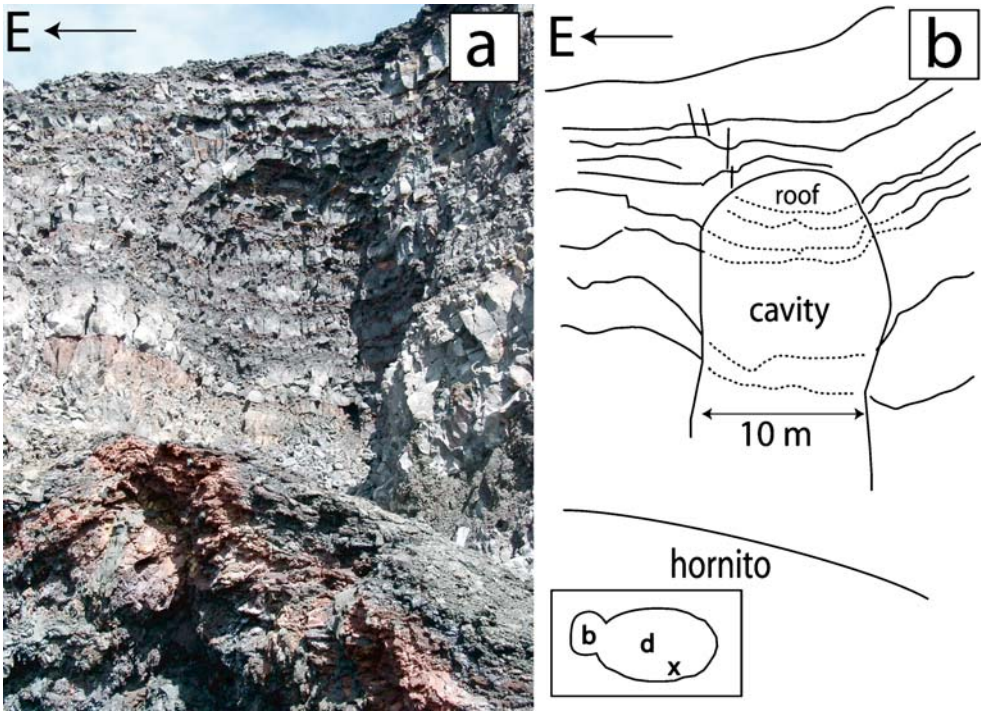

Fig. 7 **a** The Little Cavity, located in Fig 2b. Photo taken facing N180°. **b** Synthesis of observations. In the far northeast of the Southern Dolomieu Plateau a cavity was observed partially inside Dolomieu pit wall. Lava flows in the walls were continuous around the cavity, with a 10 m thick roof above. This may be further evidence of stoping and pit crater activity in the southern Dolomieu area

direction, indicating original right-lateral movement. This is in the opposite sense to the measured offset. This indicates first right-lateral shear and abrasion on the fracture and then separation with downslope tensional opening and an opposite lateral component.

The roughly northeast alignment of the fractures is an en-echelon pattern, with fractures at a high angle (70–80°) to the alignment. Such a pattern is indicative of a shear zone. In such zones, a conjugate fracture set can form, with one direction close to the shear zone orientation (*R* shears) and one at high angles (*R′* shears). *R′* shears tend to form first in diffuse shear zones; *R* shears then form with higher degrees of shear and become dominant (e.g. Freund 1974). The fractures here have a high angle and are orientated like *R′* shears. They also have the correct original shear sense for *R′* shears at this orientation if the main shear zone is left-lateral (Fig. 8b). The fractures thus indicate left-lateral displacement along a broad zone trending from the craters down the side of the steep eastern flank. The subsequent tensional opening of the fractures and the opposite sense of shear may relate to near-surface effects of the slope. Push directly from rift zone intrusions would tend to close fractures in the orientation found here and create fractures with the opposite initial shear direction. Thus, while radar interferometry data suggests that with each intrusion the whole east flank is displaced significantly (Froger et al. 2004; Fukushima et al. 2005), the deformation seen in the shear zone is probably not directly related to such effects. It is significant that the zone borders the slump structures seen on the DEM on the steep east side of the cone, as this is where a left-lateral shear zone would be expected. So, significantly, the shear zone here is probably the northwest border of the slump and is controlled by the slump and not the rift. There could be a similar opposing shear zone on the southeast side of the cone. This zone is the site of a topographic anomaly called the N120° rift zone by Bachèlery (1981) and hosts a dense group of eruptive fractures identified on the 1981 ortho-photo (Fig. 3b). However, this area has been covered by numerous recent cones and lava flows, such as the 1966 Maillard Crater, which has probably masked previous deformation. This southeast zone could be fed magma from the southern pit intrusion zone along the prominent southern N80° fissures. These intrusions could then rise up, or 'leak', into the transtensional slump boundary faults (Fig. 8c). The northeast zone, described above, is not joined to a zone of preferential magma rise and is thus less 'leaky'.

Analogue model of slumping flanks and pit formation

To test the validity of the structural observations on the flank and explore the type of structures produced on the flank of a slumping cone, a series of analogue models were carried out. The simple models consisted of a cone of sand and plaster mixture into which a layer of silicone was inserted to simulate the weak zone. The models were similar to those created by Cecchi et al. (2004) and also followed the ideas for hydrothermally altered flank instability of and van Wyk de Vries et al. (2000) and Reid et al. (2001).

The models were scaled by the same method as Cecchi et al. (2004). The cone height was 10 cm, modelling a

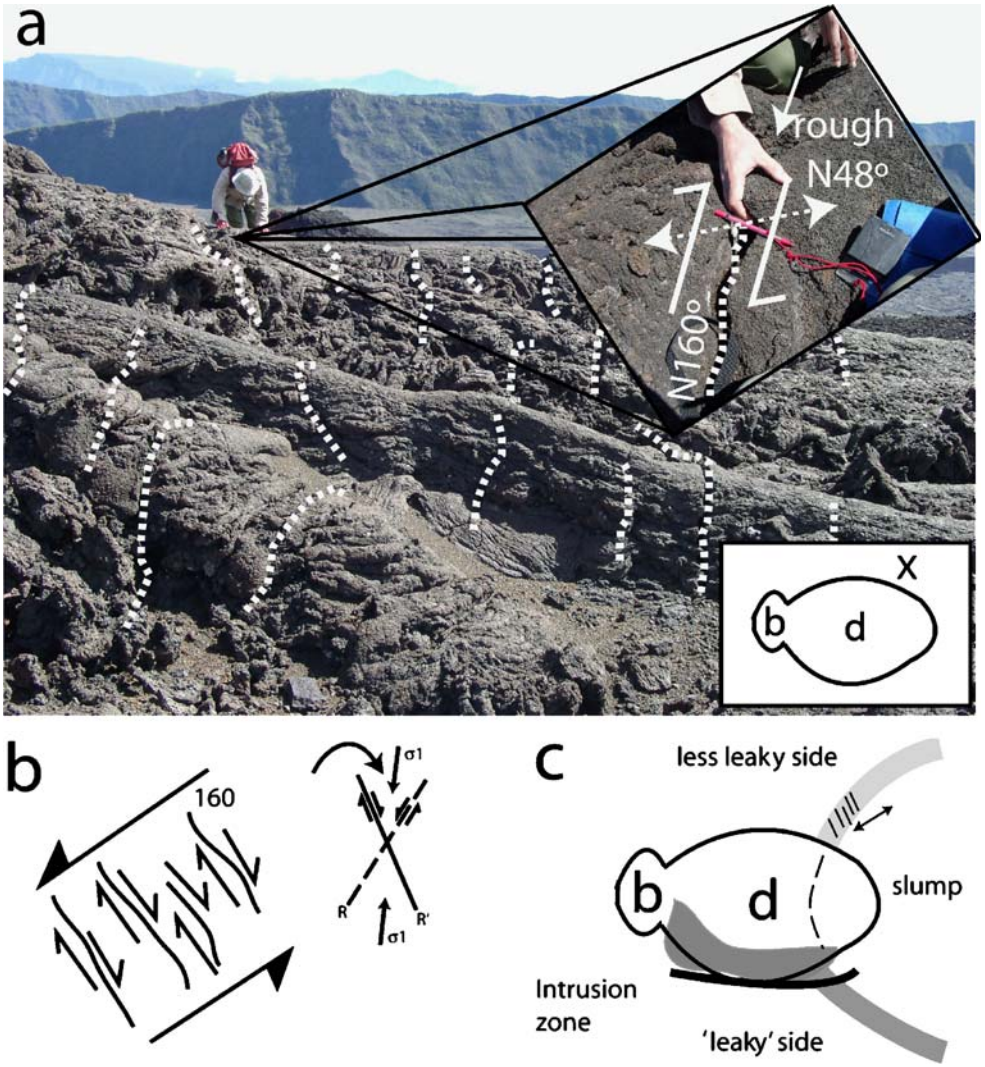

Fig. 8 **a** Shear fractures with slight right-lateral strike-slip movement on the northeast flank (see *bottom-right corner* for location map relative to Bory and Dolomieu pits, marked with an *x*). Photo taken facing N340°. Fractures displace the pahoehoe surface and are marked with *dashed white lines*. The *enlarged area* shows the orientation and opening direction of the fractures, with right-lateral displacement. **b** Structural synthesis of probable origin of fractures as *R′* shears. **c** Context of the deduced shear zone in relation to the possible slump and intrusion that form the pit system: the southern zone (*dark grey*) may be more 'leaky' than the northern zone (*light grey*) due to the presence of the southern pit intrusion zone (delineated by a *bold, dark line*)

representative natural cone of 500 m, for a scaling ratio of 2×10^{-4}. The density of the analogue material (1,200 kg m^3) was half that considered typical for lava (2,400 kg m^3) giving a scaling ratio of 0.5. Gravity is a common factor, making the stress ratio the product of the length and density ratios. Using this ratio (10^{-4}) and a cohesion of the sand-plaster brittle mixture of 50 Pa, we scaled to rock at about 10^6 Pa. Using the formula for vertical cliff height as a function of rock cohesion (Donnadieu 2000), this produces a maximum natural cliff height of about 200 m, similar to that observed in the west of Dolomieu pit.

The apparent viscosity of the weak layer could be 10^{16} to 10^{19} Pa s (van Wyk de Vries and Matela, 1998). Our usual silicone is 10^4 Pa s, giving a scaling ratio of about 10^{-12} to 10^{-15}. Scaling validity was checked by van Wyk de Vries et al. (2000) using the time ratio and reasonable natural deformation rates. With the viscosity ratio, natural fault slip rates, or flank deformation were modelled between 0.1 and 10 cm/year. This is within the range of possible slump deformation rates. More precise scaling is not possible without more detailed knowledge of the natural apparent viscosity of the hydrothermal weak layer; however, use of different viscosity silicone does not change the geometry of the structures produced, only the rate of deformation.

One main set and two subsidiary sets of experiments were carried out. For the first set, the model geometry was varied for slope angle, angular sector opening of the silicone layer, and depth of the slide layer. In all cases the models produced a slump structure with a depressed upper flank and a slightly bulging mid-flank, bounded by two shear zones with an extensional zone at the head of the structure. Maximum strike-slip movement was concentrated at the edge of the broad band of fractures. Within the curved band of fractures, a sub-parallel group was observed with orientations of N160 and N20° on the northeast and southeast flanks of the model, respectively. The early formed fractures were probably *R′* shears that were subsequently dilated by downslope extension (Fig. 9a). The interior of the slump contained a network of conjugate

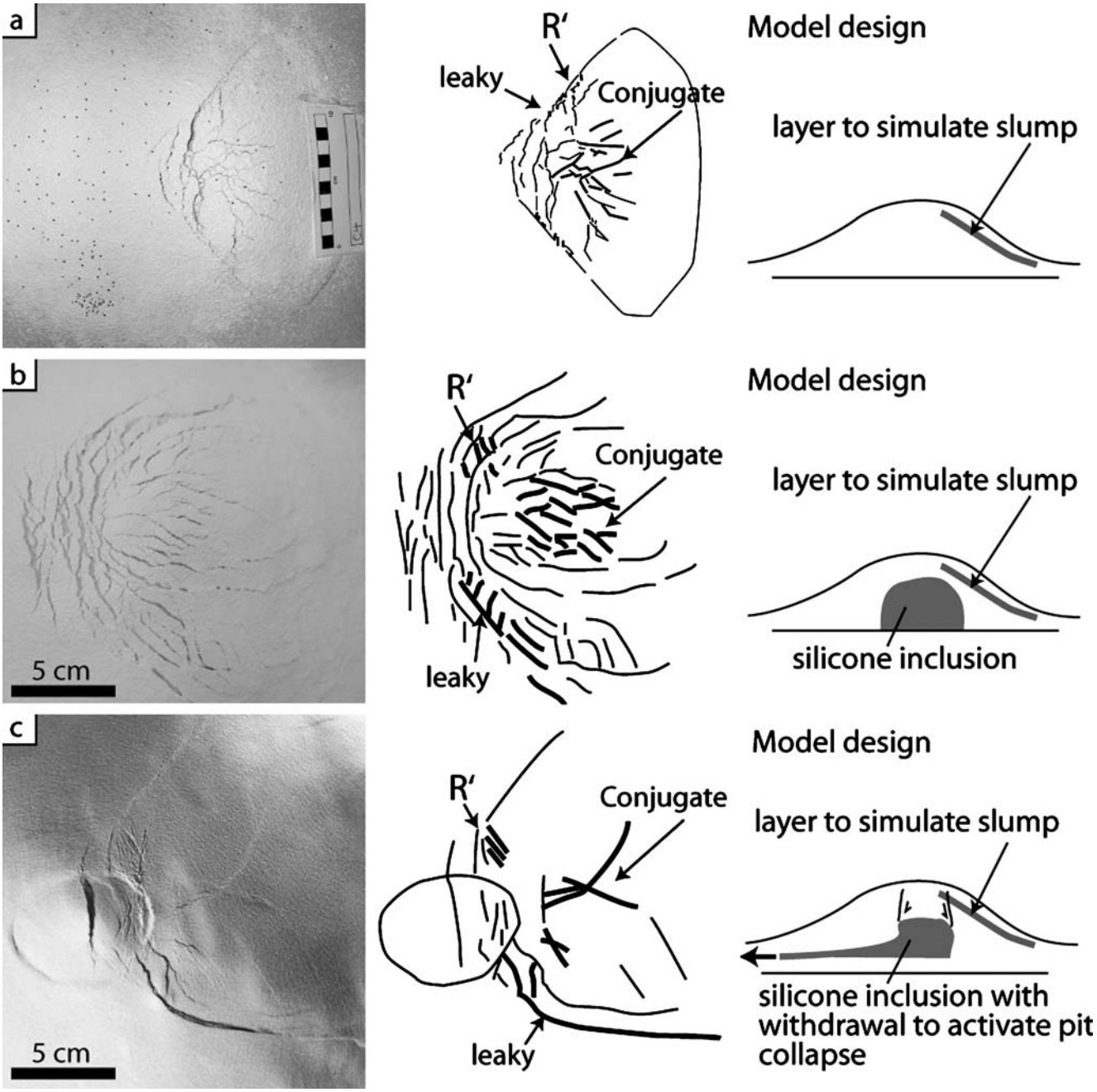

Fig. 9 Analogue models of the east flank slump with image, sketch, and model setup. **a** Model with only a slump. The model is a 20° sloped, flat-topped cone with a similar profile to Piton de La Fournaise. The cone is 10 cm high and 17 cm in radius. Note the small *R′*-like fractures that have dilated the central conjugate system. Note also that one side of the shear zone has greater extension and is therefore possibly more leaky than the other side. The *R′* shears, the conjugate set, and the 'leaky' side, developed in all models irrespective of slope, depth of decollement, or angle of opening of the silicone decollement. **b** Model with slump layer and passive inclusion to simulate the pit system, and hydrothermally active zone. **c** Model with actively subsiding pit structure and slumping layer. Both models show similar surface features. There is a summit zone of parallel fractures, a slump structure with strike-slip boundaries that have *R′* shears which evolve to tensional fractures, and a conjugate centre of the slump. Note that one strike-slip boundary increased transtension and could be a 'leaky' fault

faults. Both the *R′* and conjugate faults were best developed where the angle of the wedge of decollement was 60–120°.

A second series of models was next run with a large ductile core included next to the silicone decollement (Fig. 9b) to simulate a large hydrothermally altered core as in Cecchi et al. (2004). Features observed in these models were similar to the first set except that the head of the slump was joined to a set of radial fissures similar in orientation to the observed natural rift zones on Piton de la Fournaise.

A third series of models simulated a pit collapse (Fig. 9c) by withdrawal of silicone from the central core during slump deformation. In a similar manner to the second model series, the models produced rift fractures and the upper slump fractures joined with the pit collapse faults.

The first set of models show that a superficial decollement in the cone, such as the hydrothermally altered zone detected by electrical methods at 300 m, could produce a slump structure that has the main features observed in the field. These are the central conjugate fracture set, the boundary shear zones with early R' shears dilated by subsequent downslope movement, and the depressed upper flank. The second and third model sets show that the slump may have an important superficial effect on the geometry of structures in the pit and rift system.

Discussion

We have shown that the summit zone of Piton de la Fournaise has three major structural features: a set of pit craters and associated concentric fractures, a set of rift zones indicated by eruptive fissures and fractures, and a slumping east flank.

The pit crater system

The structural data indicate that Dolomieu is an oval collapse surrounded on three sides by outward-dipping reverse faults and a normal-reverse fault system with terraces on the western side (Figs. 10 and 11). Such a structural interpretation is in accord with the analogue experiments of Roche et al. (2001). The development of a terrace in Dolomieu after an initial collapse is a distinctive feature. This style of development is characteristic in the analogue models of a roof thickness-to-width aspect ratio of about 1:1 (Roche et al. 2001). We propose that the Enclos Velain represents the late-stage collapsed terrace as seen in the analogue experiments, which only occurs with this aspect ratio. The Bory–Dolomieu contact is thus an active normal fault that activated after the main pit formation in 1927. The block to the east of the fault then collapsed around 1933 to create the Enclos Velain terrace, elongating Dolomieu pit along an east–west axis. The normal fault is probably connected to an outward-dipping reverse ring fault that bounds the original Dolomieu collapse. Our cross-section (Fig. 10) shows that the shallower dipping fault as seen in the Roche et al. (2001) models may be located beneath the southwest section of Dolomieu, allowing a preferential rise of magma in this area. The crater morphology and direct field observations of down-stepping blocks, combined with near-continual observations of the summit from 1911 until the present day, are in agreement with the presence of a superficial normal fault in this area. Using the Roche et al. (2001) analogue model data for roof aspect ratios, the depth to the upper surface of the magma reservoir that created the Dolomieu collapse would have been approximately 1 km from the surface. This supports the possibility of a superficial magma reservoir, in accordance with previously reported seismic and deformation data (Lénat and Bachèlery 1990). This reservoir may act as a point for small intra-pit collapse nucleation. This storage location also probably acts as the initiation point of dyke intrusions into the rifts as shown by persistent volcanic activity on the surface above this area.

The rift zone system

The lack of eruptive fractures along the rift zone over the upper flanks, where fissures are more commonly N80°, may be an effect of the pit crater structure that dominates this area. The start of eruptive episodes usually begins with a seismic swarm rising below Dolomieu, followed by flank seismicity. Modelled dykes from SAR data nucleate at about 1–1.5 km depth, rising and spreading outwards (Battaglia and Bachèlery 2003; Froger et al. 2004; Fukushima et al. 2005). The modelled interferometry data gives a dike initiation depth that is similar to that of our estimated pit crater magma storage zone proposed using our structural data. This evidence is in strong agreement for the collapse model. The pit crater provides a reason for the lack of rift dykes at the summit: that is the upper 1 km is dominated by the pit structure and only as the dykes penetrate the outer flanks do they significantly affect the surface. The N10 and N170° rift zones may also initially be controlled near the surface by the slumping east flank; however, slumping may be more shallow than the dyking and, as it extends much further out than the summit cone, any influence must be localized to the summit. The large-scale arcuate shape of the rift zones may be related to the stress system of an island-scale spreading or slumping effect on Piton de la Fournaise as suggested for Canary rift zones (Walter et al. 2005).

The slumping system

The morphology of the east flank of Piton de la Fournaise is strongly indicative of a slumping region (Fig. 4). The overall east flank profile is similar to that described for flank spreading by Cecchi et al. (2004). At the base of the central east flank (approximately 2,300 m altitude), we found open fractures perpendicular to the slope. This zone may be the toe of the slumping structure, where bulging creates tension fractures. A slump origin is supported by the presence of a developing strike-slip zone on the northeast flank. This is probably the northern boundary of the slump. There is also a

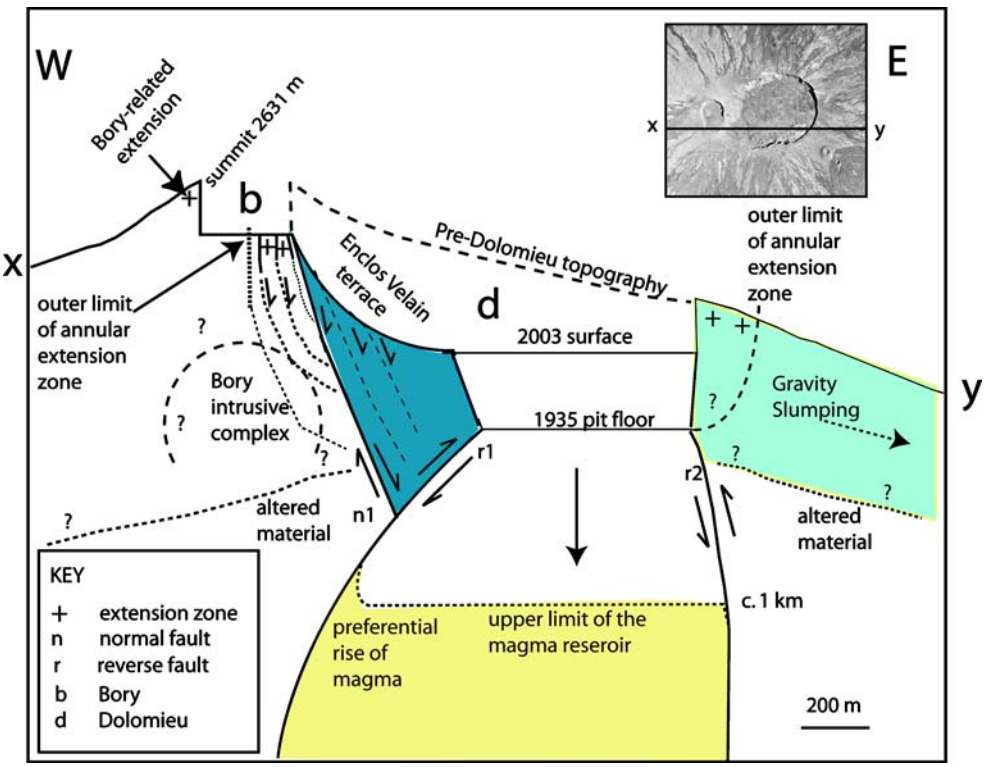

Fig. 10 East–west schematic cross-section showing the envisaged sub-surface fault system, slumping on the east flank, and a surface annular extension zone. The storage depth is assumed to be 1 km with preferential rise of magma along the south and west areas of Dolomieu. This contains the Enclos Velain block (marked as *dark grey*), bound by a normal fault which connects to a deeper reverse ring fault. The eastern flank is slumping by gravity and may be sliding on a weak layer delineated by the *upper part* of the hydrothermal system

probable southern side to the slump marked by an area of fissures that may be connected to the N120° rift zone of (Bachèlery 1981), termed here the 'leaky' strike-slip boundary (Figs. 8 and 9). The conjugate pattern of fissures on the east flank indicates a near-surface down-slope σ 1 (defined as the maximum compressive stress) and concentric stretching σ 3 (defined as the minimum compressive stress). Such a pattern has been reproduced in our analogue experiments. In all experiments, one side of the slump had a greater transtensional component that could lead to a 'leaky' boundary which allows preferential magma rise. This could be the case for the southeastern side of the slump and the N120° rift feature. These analogue models are a simplification of the possible mechanisms that can cause fracturing on Piton de la Fournaise, neglecting pit crater collapse and dyke intrusion. However, they do contain all of the main structural features seen in the field. In the models, the presence of tensional faults behind the head of the slide suggests that a slip surface could have an influence on rift zone location and that there could be a feedback relationship between slumping of the east flank and rift zone 'push.' Such a relationship between rift zones and slumps has been suggested by other analogue experiments (e.g. Walter et al. 2005).

A structural model for Piton de la Fournaise summit

The morphological study, field investigation, and comparison with analogue results leads us to propose an integrated structural model for the summit region of Piton de la Fournaise (Figs. 10, 11 and 12). The pit craters are the controlling structures in the central and summit region. The concentric fracture network forms a rough outer limit to the dominant pit structure. The annular extension zone is similar to that seen in pit crater analogue experiments (Roche et al. 2001). This zone allows us to put a limit on the sub-surface dimensions of the ring fault system.

The eruptive fissures follow a complex subsurface network of weaknesses partially controlled by dyke intrusion mechanics and intrusion position relative to the summit cone. They form a rift zone of concentrated fissures that appears strongly outside the annular extension zone but only weakly within it. On the lower north and south flanks, eruptive fissures are concentrated in two wide bands aligned with the centre of Dolomieu along a rough north–south axis. Higher up and closer to the pit craters, eruptive fissures collect in concentric fractures. This suggests an interaction between the concentric and rift fractures around the summit cone. At the summit, the preferred strike of the eruptive fissures is N80°: almost at right angles to the north and south rift zones. The N80° direction creates an axis that is also the approximate elongation axis for Dolomieu. Around the summit both the non-eruptive and eruptive fissures follow similar preferential strikes, showing a distinct lack of fractures around a strike of N110°. It may be that this direction corresponds to an overall σ1 oriented N20° that inhibits fractures in the N110° direction. This may also be partly responsible for the east–west elongation of Dolomieu. Such an elongation process for calderas has

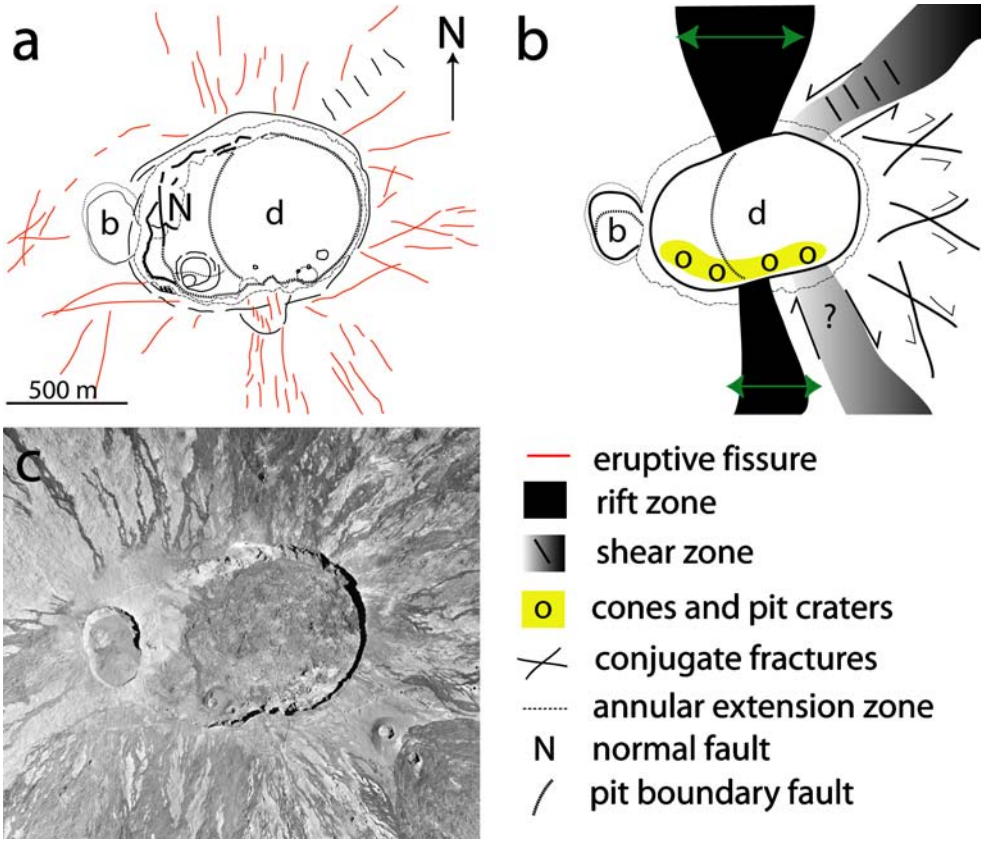

Fig. 11 **a** Plan view for the general structure of Piton de la Fournaise summit area. The main boundary faults, fractures, and eruptive fissures are marked. **b** Interpretative map of the summit area containing the rift zone, pit craters, a zone of eruptive cones and subsidence (in *light grey* with "O" symbols), the shear zone, and conjugate fractures on the east flank. **c** Aerial ortho-image taken in 1981

been previously suggested using field studies and analogue modelling (Walter and Troll 2001).

It would be reasonable to suggest that an older intrusive complex lies beneath Bory with a crystallised magma storage area and dyke network. The west flank is a more stable block within the volcano, as it is buttressed against the Enclos Fouqué caldera, possibly explaining the low amount of eruptive vents in Bory pit and its immediate surroundings. Two large, non-eruptive fractures over 1 m wide and 50 m long cut Bory with an east–west opening direction. They are both over 5 m in depth in places and show no vertical displacement. Accocella et al. (2003) demonstrated that tension fractures may undergo a transition into normal faults after a critical depth based on research on the Ethiopian rift system. This mechanism may apply to the fractures of this area and would indicate a connection with the Enclos Velain fault terrace at depth.

Small diameter (<50 m) deep intra-pit cavern collapses, such as the post-1964 La Soufriere collapse, the Little Cavity inside the south Dolomieu walls, and the 1986 and 2002 pit craters, are produced by collapses of higher roof aspect ratios (1.1–2). We interpret that the Little Cavity did not undergo total roof collapse, but remained sub-surface until the Dolomieu collapse began in 1927. A recent eruptive fissure (June 2003) lies within 25 m of the southwest Dolomieu pit wall on an east–west alignment, with a series of intra-pit scoria cones, the Little Cavity, and the 1986 pit crater to the southeast in Dolomieu pit. These features are grouped around the south and southwest sides of Dolomieu and are the sites of many small pit craters and scoria cones. This feature concentration suggests that the southwest part of the sub-surface ring fault may have a lower dip angle, with the preferential rise of magma in this area (Roche et al. 2001). Small bodies of magma can form at about 1 km depth in the breccias associated with the main collapse. The drainage of these could create voids which then migrate up to the surface. Such a process was actually observed at Masaya volcano (Rymer et al. 1998). A downward 'piston' movement can potentially create a space along the fault, providing a pathway for magma; conversely, an upward movement will tend to block the system. Intra-pit eruptions should therefore be related to pit subsidence, as observed at Masaya volcano (Rymer et al. 1998), where they tend to rise along intra-pit cavern collapses (Walker 1988).

On the eastern flank, eruptive fissures occur as conjugate fracture sets which, with the depression and the strike-slip bounding fractures, indicate that this area is spreading to the east. Self-potential measurements in Dolomieu show a negative anomaly along the eastern border of the pit (Lénat et al. 2000), which fits exactly with the extensions of the boundary shear zone. This is a cold area of low heat flow, which may be caused by an isolating layer at the base of the slump and possibly a channelling of cold meteoric water down the slump (Labazuy et al. 2004a,b).

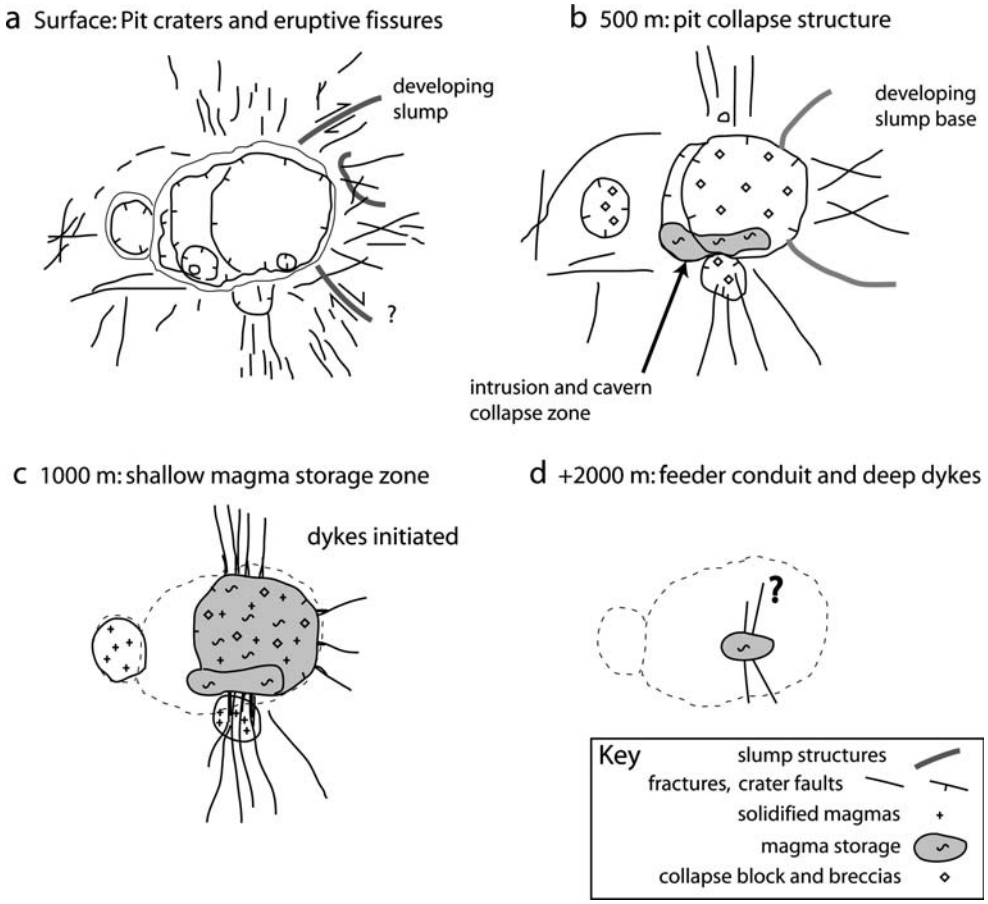

Fig. 12 **a** Structural summary for the summit of Piton de la Fournaise. Map view summary for a slice across each depth level is given. **b** Superficial slumping and pit crater structures dominate the upper 500 m, beneath which lie intrusions and cavern collapse areas. **c** At around 1,000 m the summit contains a shallow magma storage zone where the modelled dykes originate. **d** The feeder conduit and deeper dykes lie around 2,000 m, beneath the pit crater structures

We propose that the upper 2 km of the summit can be separated in to four layers (Fig. 12). The upper 500 m is governed by pit crater subsidence and superficial slumping (Fig. 12a). Pit crater breccia and chaotic deposits are found around 500 m depth with infilled caverns and intrusion pathways (Fig. 12b). Around 1,000 m depth, a shallow magma storage zone is found at the base of the pit crater structure where dykes are initiated (Fig. 12c). Magma may be guided into the rift zones (the most common direction) or towards the east, where they are captured by the slump and probably guided up pre-existing fractures. Feeder conduit and deep dykes are located around 2,000 m depth and below (Fig. 12d).

Conclusions

Eruptive activity in pit craters dominates the summit region of Piton de La Fournaise where collapse structures continue to form after eruptive events. Intrusions originating in the magma storage system at about 1 km below Dolomieu pit either: (1) feed into the rift zones (N10 and N170°) and bypass the summit; (2) are intruded with a dominant N80° orientation around the summit; or (3) erupt through the southern pit border. Gravity-driven slumping is occurring on the eastern flank, sliding on a surface at around a depth of 300 m and marked by self-potential anomalies in the upper region of the hydrothermal system (Lénat et al. 2000). The slumping intersects the east side of Dolomieu and has controlled the location of eruptive fissures in this area, by sapping magma from the southern intrusion zone along N80° fractures into the southern slump, or by controlling rise on pre-existing conjugate structures. Dykes initiated below this area follow the pre-existing fracture network, being passively guided to the surface.

Our model has demonstrated that the pits, rifts, and slumps are interactive magmatic- and gravity-driven features on the summit. Future work on the east flank may reveal more evidence of rift-slump interaction near the summit pit craters. The model presented here is in agreement with available deformation and geophysical data. Furthermore, the model allows for predictions to be made about the volcano's response to different intrusive–eruptive events which can now be tested and refined using monitoring data.

Acknowledgements This work was funded by a PNRN and ACI grant to van Wyk de Vries from the CNRS. Ample assistance was given by the Observatory on Piton de La Fournaise, especially from Dr. Thomas Staudacher. This paper was significantly improved by the

helpful reviews of Dr. Francesco Mazzarini and Prof. Stephen Self, and edits from Dr. Andrew Harris. Fruitful conversations with JF Lénat and P Labazuy improved the manuscript. Thanks also to Dr. Luke Wooller for his suggestions and to Nerissa Lindenfelser for helpful comments.

References

Accocella V, Korme T, Salvini F (2003) Mechanism of fault formation along the axial zone of the Ethiopian Rift. J Struct Geol 25:503–513

Bachèlery P (1981) Le Piton de la Fournaise: Etude Volcanologique, Structurale et Pétrologique. PhD thesis, University of Clermont Ferrand, France:1–257

Bachèlery P, Chevallier P, Gratier JP (1983) Volcanologie: Caractères structuraux des éruptions historiques du Piton de la Fournaise (Ile de la Réunion). C R Acad Sci Paris 296:1345–1350

Battaglia J, Bachèlery P (2003) Dynamic dyke propagation deduced from tilt variations preceding the March 9, 1998, eruption of the Piton de la Fournaise volcano. J Volcanol Geotherm Res 120:289–310

Bory de St. Vincent (1804) Voyages dans les quatre principales iles des mers d'Afrique, Paris

Cecchi E, van Wyk de Vries B, Lavest JM, Harris A, Davies M (2003) N-view reconstruction: a new method for morphological modelling and deformation measurement in volcanology. J Volcanol Geotherm Res 123:181–201

Cecchi E, van Wyk de Vries B, Lavest J-M (2004) Flank spreading and collapse of weak-cored volcanoes. Bull Volcanol 67:72–91

Delorme H, Bachèlery P, Blum PA, Cheminée JL, Delarue JF, Delmond JC, Hirn A, Lepine JC, Vincent PM, Zlotnicki J (1989) March 1986 eruptive episodes at Piton de la Fournaise volcano (Reunion Island). J Volcanol Geotherm Res 36:199–208

Donnadieu F (2000) Déstabilisation des édifices volcaniques par les cyptodômes: Modélisation analogique et approche numérique. PhD thesis, University of Clermont-Ferrand, France:1–256

Freund R (1974) Kinematics of transform and transcurrent faults. Tectonophysics 21:93–134

Froger J-L, Fukushima Y, Briole P, Staudacher T, Souriot T, Villeneuve N (2004) The deformation field of the August 2003 eruption at Piton de la Fournaise, Reunion Island, mapped by ASAR interferometry. Geophys Res Lett 31:L14601, DOI 10.1029/2004GL020479

Fukushima Y, Cayol V, Durand P (2005) Finding realistic dike models from interferometric synthetic aperture radar data: the February 2000 eruption at Piton de la Fournaise. J Geophys Res 110: B03206, DOI 10.1029/2004JB003268

Gillot P-Y, Nativel P, Condomines M (1990) Geochronologie du Piton de la Fournaise. In: Lénat J-F (ed) Le Volcanisme de La Réunion. Centre de Recherches Volcanologiques, Clermont Ferrand, France: 243–256

Kelfoun K (1999) Processus de croissance et de déstabilisation des dômes de lave du volcan Merapi (Java centrale, Indonésie). PhD thesis, University of Clermont-Ferrand, France:1–261

Kornprobst J, Boivin P, Lénat J-F, Bachèlery P, Bonneville A, Dupont P, Lecointre J, Seidel J-L, Thomas P, Vincent P (1984) Le Piton de la Fournaise, ile de la Reunion. In: Prévision et Surveillance des Eruptions Volcaniques. Proceedings, Clermont Ferrand, France:75–82

Labazuy P, Charbonnier S, Staudacher T, Oehler J-F (2004a) New insights on the December 2002 pit crater at Piton de la Fournaise from self potential and GPS surveys. EGU 1st General Assembly, Nice, France, 25–30 April 2004, EGU04-03226

Labazuy P, Saracco G, Lénat J-F, Charbonnier S, Mauri G (2004b) EM Tomography and modeling of the hydrothermal system of Piton de la Fournaise, Reunion Island. IAVCEI General Assembly, Pucon, Chile, 15–19 November 2004

Lacroix A (1936) Le Volcan actif de l'ile de La Réunion et ses produits. Gauthier Villars (ed) Paris, pp 1–297

Lénat J-F, Bachèlery P (1990) Structure et fonctionnement de la zone centrale du Piton de la Fournaise. In: Lénat J-F (ed) Le Volcanisme de La Réunion. Centre de Recherches Volcanologiques, Clermont Ferrand, France:257–296

Lénat J-F, Fitterman D, Jackson DB, Labazuy P (2000) Geoelectrical structure of the central zone of Piton de la Fournaise volcano (Réunion). Bull Volcanol 62:75–89

Lénat J-F, Bachèlery P, Desmulier F (2001) Genese du champ de lave de l'Enclos Fouqué: une éruption d'envergure exceptionnel du Piton de la Fournaise (Réunion au 18ieme siècle). Bulletin de la Société Géologique de France 172:177–188

Murray JB (1988) The influence of loading by lavas on the siting of volcanic eruption vents on Mt Etna. J Volcanol Geotherm Res 35:121–139

Okubo CH, Martel SJ (1998) Pit crater formation on Kilauea volcano, Hawaii. J Volcanol Geotherm Res 86:1–18

Reid ME, Sisson TW, Brien DL (2001) Volcano collapse promoted by hydrothermal alteration and edifice shape, Mount Rainier, Washington. Geology 29:779–782

Roche O, van Wyk de Vries B, Druitt TH (2001) Sub-surface structures and collapse mechanisms of summit pit craters. J Volcanol Geotherm Res 105:1–18

Rowland SK, Garbeil H (2000) Slopes of oceanic basalt volcanoes. Geophys Monogr 116:223–247

Rymer H, van Wyk de Vries B, Stix J, Williams-Jones G (1998) Pit crater structure and processes governing persistent activity at Masaya volcano, Nicaragua. Bull Volcanol 59:345–355

Stieltjes L (1985) Carte des coulées historiques du volcan de la Fournaise (Ile de la Réunion, Ocean Indien). Bureau de Recherches Géologiques et Minières

van Wyk de Vries B, Matela R (1998) Styles of volcano-induced deformation: numerical models of substratum flexure, spreading and extrusion. J Volcanol Geotherm Res 81:1–18

van Wyk de Vries B, Kerle N, Petrey D (2000) A sector collapse forming at Casita, Nicaragua. Geology 28:167–170

Walker GPL (1988) Three Hawaiian calderas: an origin through loading by shallow intrusions? J Geophys Res 93:14773–14784

Walter TR, Troll VR (2001) Formation of caldera periphery faults, an experimental study. Bull Volcanol 63:191–203

Walter TR, Troll VR, Cailleau B, Belousov AB, Schmincke H-U, Amelung F, Bogaard Pvd (2005) Rift zone reorganization through flank instability in ocean island volcanoes: an example from Tenerife, Canary Islands. Bull Volcanol 67:281–291